Contents lists available at ScienceDirect

BBA - Molecular Basis of Disease

journal homepage: www.elsevier.com

Iron overload inhibits osteogenic commitment and differentiation of mesenchymal stem cells via the induction of ferritin

Enikő Balogh,[a] Emese Tolnai,[a] Béla Nagy, Jr. [b] Béla Nagy,[c] György Balla,[c] József Balla,[a] Viktória Jeney [a, *]

[a] Department of Internal Medicine, Faculty of Medicine, University of Debrecen, 98. Nagyerdei Krt., 4012 Debrecen, Hungary
[b] Department of Laboratory Medicine, Faculty of Medicine, University of Debrecen, 98. Nagyerdei Krt., 4012 Debrecen, Hungary
[c] Department of Pediatrics, Faculty of Medicine, University of Debrecen, 98. Nagyerdei Krt., 4012 Debrecen, Hungary

ARTICLE INFO

Article history:
Received 16 February 2016
Received in revised form 2 June 2016
Accepted 5 June 2016
Available online xxx

Keywords:
Human mesenchymal stem cell
Osteogenic differentiation
Iron
Ferritin
Runx2

ABSTRACT

Osteogenic differentiation of multipotent mesenchymal stem cells (MSCs) plays a crucial role in bone remodeling. Numerous studies have described the deleterious effect of iron overload on bone density and microarchitecture. Excess iron decreases osteoblast activity, leading to impaired extracellular matrix (ECM) mineralization. Additionally, iron overload facilitates osteoclast differentiation and bone resorption. These processes contribute to iron overload-associated bone loss. In this study we investigated the effect of iron on osteogenic differentiation of human bone marrow MSCs (BMSCs), the third player in bone remodeling.

We induced osteogenic differentiation of BMSCs in the presence or absence of iron (0–50 μmol/L) and examined ECM mineralization, Ca content of the ECM, mRNA and protein expressions of the osteogenic transcription factor runt-related transcription factor 2 (Runx2), and its targets osteocalcin (OCN) and alkaline phosphatase (ALP). Iron dose-dependently attenuated ECM mineralization and decreased the expressions of Runx2 and OCN. Iron accomplished complete inhibition of osteogenic differentiation of BMSCs at 50 μmol/L concentration. We demonstrated that in response to iron BMSCs upregulated the expression of ferritin. Administration of exogenous ferritin mimicked the anti-osteogenic effect of iron, and blocked the upregulation of Runx2, OCN and ALP. Iron overload in mice was associated with elevated ferritin and decreased Runx2 mRNA levels in compact bone osteoprogenitor cells. The inhibitory effect of iron is specific toward osteogenic differentiation of MSCs as neither chondrogenesis nor adipogenesis were influenced by excess iron. We concluded that iron and ferritin specifically inhibit osteogenic commitment and differentiation of BMSCs both in vitro and in vivo.

1. Introduction

Mesenchymal stem cells (MSCs) are multipotent stromal cells, with the capability to differentiate into various mesenchymal lineages, including but not limited to osteoblasts, chondrocytes and adipocytes [1]. Numerous signaling cascades were explored driving the commitment, and differentiation of MSCs toward the different lineages [2].

Osteogenic differentiation of MSCs is driven by many secreted differentiation factors, including transforming growth factor-beta 1, fibroblast growth factor, bone morphogenetic protein, wingless proteins, Indian hedgehog, which all converge on the master osteogenic transcription factor, runt-related transcription factor 2 (Runx2) [3]. The crucial importance of Runx2 in osteogenic differentiation is highlighted by the finding, that Runx2 deficient mice completely lack differentiated osteoblasts resulting impaired bone formation, and die shortly after birth [4,5]. Runx2 regulates the transcription of the major bone-specific proteins, such as osteocalcin (OCN), osteopontin, bone sialoprotein, α1 type I collagen and alkaline phosphatase (ALP), those expression is required for proper bone formation [6]. Recently, the role of reactive oxygen species (ROS) in osteogenesis, as a common denominator of the diverse osteogenic signaling pathways, has been established [7]. Studies revealed that tightly regulated levels of ROS are critical in osteogenic differentiation of MSCs [7].

Hemochromatosis, the accumulation of excess iron in the body tissues, damages different organs, particularly the liver, the pancreas and the heart. Several reports described low bone density, osteoporosis and/or osteopenia in patients with different forms of hemochromatosis [8–11]. Supporting this notion, both pharmacological and genetic provocation of iron overload was shown to be associated with bone abnormalities in rodent models of hemochromatosis. For example, intraperitoneal injection of ferric iron results in bone loss [12,13]. Additionally, a bone phenotype of osteoporosis with low bone mass and alteration of the bone microarchitecture has been described in a mouse model of genetic hemochromatosis [14]. Recently, hepcidin, the liver-derived regulator of iron homeostasis has been also identi-

Abbreviations: ALP, alkaline phosphatase; BMP2, bone morphogenetic protein 2; BMSCs, bone marrow-derived mesenchymal stem cells; CM-H_2DCFDA, 5-(and-6)-chloromethyl-2′,7′-dichlorodihydro-fluorescein di-acetate, acetyl ester; ECM, extracellular matrix; Fabp4, fatty acid-binding protein 4; FtH, ferritin heavy chain; FtL, ferritin light chain; HBSS, Hank's balanced salt solution; HPRT, hypoxanthine-guanine phosphoribosyl transferase; MSCs, mesenchymal stem cells; OCN, osteocalcin; OPG, osteoprotegerin; OPCs, osteoprogenitor cells; Pi, inorganic phosphate; RANKL, receptor activator of nuclear factor-kappa B ligand; ROS, reactive oxygen species; Runx2, runt-related transcription factor 2; VSMCs, vascular smooth muscle cells

* Corresponding author at: Vascular Immunology Research Group, Department of Internal Medicine, Faculty of Medicine, University of Debrecen, Nagyerdei krt. 98, 4012 Debrecen, Hungary.
Email address: jeneyv@belklinika.com (V. Jeney)

http://dx.doi.org/10.1016/j.bbadis.2016.06.003
0925-4439/

fied as a factor influencing bone physiology. Lack of hepcidin triggers severe tissue iron overload that is associated with low bone mass, and altered bone microarchitecture [15,16].

Excess iron generates oxidative stress, characterized by an increase in the steady state level of ROS, which mediates cellular and tissue damage, that is believed to be the major pathogenic factor in iron overload diseases [17]. To counteract with iron toxicity, excess iron is sequestered by ferritin, the major iron storage molecule. Ferritin shell is made up of 24 subunits of two types, heavy (H) and light (L), and can accommodate as much as 4500 Fe^{3+} ions in a safe and bioavailable form [18,19]. The H subunit exhibits ferroxidase activity that promotes oxidation of Fe^{2+} into Fe^{3+}, while the L subunit plays a role in iron nucleation, and long-term iron storage [18,20]. The expression of ferritin subunits are tightly regulated by iron, both the transcriptional and translational levels [21–23].

Bone is an active tissue that is continuously being reshaped, in a process called remodeling, in which osteoclasts resorb bone tissue, whereas osteoblasts deposit new bone tissue. The cellular mechanism behind the detrimental role of excess iron in bone physiology can be the consequence of facilitated differentiation, and increased activity of osteoclasts, or decreased activity of osteoblasts, or both. Iron has been shown to facilitate osteoclast differentiation [24]. Also, osteoclast activity is increased in thalassemia major patients, but this was found to be rather associated with inflammation, than increased iron stores [25]. Previously, we showed that iron potently inhibited matrix mineralization of mature osteoblasts [26]. Iron-mediated inhibition of osteoblast matrix mineralization relied on decreased phosphate uptake, and the downregulation of Runx2, the osteoblast-specific transcription factor and its target transcripts: OCN and ALP [26]. Ferritin, the iron-regulated, iron-storage protein, mimicked the inhibitory effect of iron on matrix mineralization of mature osteoblasts [26].

Osteoblasts derive from mesenchymal progenitor cells, which migrate to the site of injury, proliferate and differentiate [27]. Osteogenic potential of these bone marrow-derived MSCs (BMSCs) is of crucial importance for proper remodeling and/or healing, which is highlighted by the recent discovery, that osteoporosis is associated with low osteogenic potential of circulating MSCs [28]. This prompted us to examine the role of iron in MSC osteogenic commitment, and differentiation.

2. Materials and methods

2.1. Materials

Unless otherwise specified all reagents were from Sigma-Aldrich Co. (St. Louis, MO, USA).

2.2. Cell culture

Human BMSCs derived from 2 different adult donors of Caucasian origin were obtained from ScienCell Research Laboratories (Carlsbad, CA, USA). Cells were maintained in DMEM (high glucose), containing 10% FBS (Gibco, Grand Island, NY, USA), 10,000 U/mL penicillin, 10 mg/mL streptomycin, 25 μg/mL amphotericin B, and 1 mmol/L sodium pyruvate. Cells were grown to confluence, and used from passages 4 through 7. Iron was introduced as ferrous sulfate. Ferritin was introduced as holo-ferritin (Ft).

2.3. Mice

All experiments were performed in compliance with institutional (Institutional Ethics Committee, University of Debrecen) and national guidelines. Ten C57BL/6 mice (8–10 weeks old, male) were randomly divided into two groups. The iron-overload group was injected intraperitoneally with iron-dextran (200 mg/kg body weight, 3-times, every other day), while control mice were treated with PBS. Mice were sacrificed with CO_2 inhalation and perfused with 5 mL of ice-cold PBS, tibia and femur were harvested for analysis.

2.4. Isolation of compact bone osteoprogenitor cells (OPCs)

OPCs were isolated from compact bones as described by Zhu et al. [29]. Briefly, after harvesting and cleaning the tibia and femur, the epiphyses were removed. To release bone marrow, bones were fragmented and agitated in a mortar containing ice cold PBS supplemented with 2% FBS and 1 mmol/L EDTA. This washing step was repeated 5 times, and the bone-marrow free bones were digested in 0.25% Collagenase Type I (5 min, RT). Then the bones were chopped into 1–2 mm pieces and digested for an additional 45 min at 37 °C. Finally the bone chips were washed, and the obtained suspension was filtered through a 70 μm cell strainer and centrifuged (300*g*, 10 min, RT). Harvested cells were used to isolate RNA immediately.

2.5. Induction of osteogenic differentiation

At confluence, BMSCs were switched to osteogenic medium, which was prepared by adding inorganic phosphate (Pi) (0–3 mmol/L) and Ca at the form of $CaCl_2$ (0–1.2 mmol/L) to the growth medium. Both growth medium and osteogenic medium were changed in every other day. Unless otherwise specified, we used an osteogenic medium that was supplemented with 3 mmol/L Pi and 1.2 mmol/L Ca. Alternatively, osteogenic differentiation was induced by dexamethasone (0.1 μmol/L), ascorbic acid (50 μmol/L) and β-glycerol-phosphate (2 mmol/L) for 14 days. When appropriate, cycloheximide (CHX) was used to inhibit protein synthesis at a concentration of 10 μg/mL.

2.6. Induction of chondrogenic differentiation

To induce chondrogenic differentiation, BMSCs were cultured in chondrogenic medium, containing StemPro Chondrogenesis Supplement (Gibco, Grand Island, NY, USA) and gentamicin (10 mg/mL) for 14 days.

2.7. Induction of adipogenic differentiation

To induce adipogenic differentiation, confluent BMSCs were cultured in adipocyte differentiation medium, containing StemPro Adipocyte Supplement (Gibco, Grand Island, NY, USA) and gentamicin (10 mg/mL) for 3 weeks.

2.8. Alizarin red staining

After washing with PBS, the cells were fixed in 4% paraformaldehyde and rinsed with deionized water thoroughly. Cells were stained with Alizarin Red S solution (2%, pH 4.2) for 20 min at room temperature. Excessive dye was removed by several washes in deionized water. Extracellular Ca deposition was stained in red color using Alizarin Red S dye.

2.9. Alcian blue staining

Alcian blue staining was performed with NovaUltra Special Stain Kit (IHC World, Ellicott City, MD, USA) according to the manufacturer's instructions.

2.10. Oil Red O staining

After washing with PBS, the cells were fixed in 4% paraformaldehyde and rinsed with deionized water thoroughly. Isopropanol (60%) was added to the cells for 5 min, followed by the addition of Oil Red O working solution (0.18% in 60% isopropanol) for 5 min. Excessive dye was removed by several washes in water.

2.11. Quantification of Ca deposition

Cells grown on 96-well plates were washed twice with PBS, and decalcified with HCl (0.6 mol/L) for 30 min at room temperature. Ca content of the HCl supernatants was determined by QuantiChrome Calcium Assay Kit (Gentaur, Kampenhout, Belgium). Following decalcification, cells were washed twice with PBS, and solubilized with a solution of NaOH (0.1 mol/L) and sodium dodecyl sulfate (0.1%), and protein content of samples were measured with BCA protein assay kit (Pierce Biotechnology, Rockford, IL, USA). Ca content of the cells were normalized to protein content, and expressed as μg/mg protein.

2.12. Intracellular phosphate measurement

After 1 day of culture, cells were washed twice with PBS and solubilized with 1% Triton-X100. Cell lysates were assayed for inorganic phosphate using QuantiChrome Phosphate Assay Kit (Gentaur, Kampenhout, Belgium).

2.13. Quantification of OCN

For OCN detection, the ECM of cells grown on 6-well plates was dissolved in 100 μL of EDTA (0.5 mol/L, pH 6.9). OCN content of the EDTA-solubilized ECM samples was quantified by an enzyme-linked immunosorbent assay (ELISA) (eBioscience, San Diego, CA, USA).

2.14. Measurement of ALP activity

Cells grown on 96-well plates were treated with osteogenic medium for 7 days. Then cells were lysed and 35 μL cell lysate was mixed with 130 μL of ALP Yellow Liquid Substrate. Formation of *p*-nitrophenol was followed at 405 nm for 30 min at 37 °C. Maximum slope of the kinetic curves was used for calculation of ALP activity which was then normalized to protein content.

2.15. Cell viability assay

Cell viability was determined by the MTT assay as previously described [30]. Briefly, cells were cultured and treated in 96-well plates for the indicated time. Then cells were washed with PBS, and 100 μL of 3-[4,5-dimethylthiazol-2-yl]-2,5-diphenyl-tetrazolium bromide (0.5 mg/mL) solution in HBSS was added. After a 4-hour incubation the MTT solution was removed, formazan crystals were dissolved in 100 μL of DMSO and optical density was measured at 570 nm.

2.16. Quantitative RT-PCR

RNA was isolated from cells using TRIzol (RNA-STAT60, Tel-Test Inc., Friendswood, TX, USA) according to the manufacturer's protocol. Two micrograms of RNA were reverse transcribed to cDNA with High-Capacity cDNA Reverse Transcription Kits (Applied Biosystems, Waltham, MA, USA). Quantitative real-time PCR was performed using iTaq Universal Probes Supermix (BioRad Laboratories, Hercules, CA, USA) and predesigned primers and probes (TaqMan® Gene Expression Assays) to detect *Fabp4* (fatty acid-binding protein 4) (Hs.391561), *Runx2* (Hs.535845, Mm.00850707), *FtH* (Mm.00501584), *GAPDH* (Mm.99999915) and *HPRT* (hypoxanthine-guanine phosphoribosyl transferase) (Hs.412707). Relative mRNA expressions were calculated with the ΔΔCt method using *HPRT* or *GAPDH* as internal control.

2.17. Western blot

To evaluate protein expressions, cell lysates were run on 10% SDS-PAGE. Western Blotting was performed with the use anti-Runx2 antibody and anti-human ferritin heavy (FtH) and light (FtL) chain antibodies (Santa Cruz Biotechnology, Inc., Dallas, TX, USA) at 1:200 dilution, anti-aggrecan and anti-fatty acid binding protein 4 (Fabp4) antibodies (ProteinTech, Chicago. IL, USA), at 1:500 dilution, followed by HRP-labeled anti rabbit IgG antibody (Amersham Biosciences Corp., Piscataway, NJ, USA). Antigen-antibody complexes were visualized with the horseradish peroxidase chemiluminescence system (Amersham Biosciences Corp., Piscataway, NJ, USA). After detection, the membranes were stripped and reprobed for GAPDH using anti-GAPDH antibody at a dilution of 1:1000 (Novus Biologicals, Littleton, CO, USA). Results were quantified by using Alpha DigiDoc RT (Alpha Innotech, San Leandro, CA, USA) quantification system.

2.18. Intracellular ROS measurement

ROS production was monitored by using the 5-(and-6)-chloromethyl-2′,7′-dichlorodihydro-fluorescein di-acetate, acetyl ester (CM-H_2DCFDA) assay (Life Technologies, Carlsbad, CA, USA). After a 24-hour treatment cells were washed with PBS and loaded with CM-H_2DCFDA (10 μmol/L, 30 min, in the dark). Cells were washed thoroughly and fluorescence intensity was measured in every 30 min for 3 h applying 488 nm excitation and 533 nm emission wavelengths. In some experiments ROS was scavenged by *N*-acetyl cysteine (NAC, 0.5 mmol/L).

2.19. Statistical analysis

Data are shown as mean ± S.D. Statistical analysis was performed by ANOVA test followed by post hoc Newman-Keuls test for multiple comparisons. A value of $p < 0.05$ was considered significant.

3. Results

3.1. Pi and Ca induce mineralization of BMSCs in a dose-dependent manner

The mechanisms of BMSC osteogenic differentiation and VSMC osteoblastic trans-differentiation shares similarities including common triggers. First we tested whether Pi and Ca, the well-known and physiologically relevant triggers of osteogenic trans-differentiation of

VSMCs induce osteogenic differentiation of BMSCs. At confluence growth media was supplemented with different concentrations of Pi (0–3 mmol/L) and Ca (0–1.2 mmol/L) and cells were cultured for 5 days. Alizarin red staining revealed that while Pi and Ca alone did not induce ECM mineralization, when these triggers were applied together a dose-dependent mineralization of the ECM occurred, suggesting a synergistic effect of Pi and Ca in inducing ECM calcification (Fig. 1A). We observed a slight but significant increase in the Ca content of the ECM when the growth media was supplemented with 2 mmol/L Pi, and 0.6 mmol/L Ca (Fig. 1B). Higher concentrations of Ca and Pi induced a more robust increase in the Ca content of ECM (Fig. 1B). Importantly, these concentrations of Ca and Pi did not influence cell viability that was assessed by MTT assay (Fig. 1C). Based on these results, we used an osteogenic medium supplemented with 3 mmol/L Pi and 1.2 mmol/L to induce osteogenic differentiation of BMSCs throughout this paper. Because the active, cell-mediated nature of ECM mineralization in VSMCs was questioned for decades, we wanted to be sure that Pi and Ca-induced mineralization is a cell-mediated process in BMSCs. To investigate this, we supplemented the osteogenic medium with the protein synthesis inhibitor, CHX. We found that CHX completely inhibited ECM mineralization, proving that de novo protein synthesis is required for ECM mineralization and Ca deposition in BMSCs (Fig. 1D).

3.2. Iron inhibits Pi and Ca-induced mineralization of BMSCs in a dose-dependent manner

Previously we showed that iron inhibits osteoblast activity as well as Pi-induced osteogenic trans-differentiation of VSMCs [26,31]. To examine whether iron can inhibit Pi and Ca-induced osteogenic differentiation of BMSCs, we cultured the cells in osteogenic medium in the presence (1–50 μmol/L), or absence of iron. As revealed by alizarin red staining, iron caused a dose-dependent attenuation of mineralization, leading to complete inhibition at the concentration of 50 μmol/L (Fig. 2A). Next, we examined the effect of iron on Ca content of the ECM. Iron caused a dose-dependent decrease in the Ca content of the ECM (Fig. 2B). At the concentration of 50 μmol/L, iron lowered Ca content of the ECM of stimulated cells down to the level of non-stimulated cells (Fig. 2B).

3.3. Iron down-regulates the expression of Runx2 and its downstream target OCN and ALP

Runx2 is the master transcription factor of osteogenesis therefore next we examined the effect of iron on the level of Runx2. Osteogenic stimulation induced an about 1.6-fold increase in Runx2 mRNA level that was attenuated by iron (Fig. 3A). Importantly, iron at the concentration of 50 μmol/L decreased the level of Runx2 mRNA down to the level of unstimulated cells (Fig. 3A). Parallel with changes in mRNA levels, osteogenic stimulation increased the protein expression of Runx2 by 1.6-fold (Fig. 3B). Iron inhibited osteogenic stimuli-induced upregulation of Runx2. Moreover, iron at the concentration of 50 μmol/L decreased Runx2 protein expression well below the Runx2 expression of control cells (Fig. 3B). Next, we determined the level of OCN, a bone-specific protein which expression is under the control of Runx2. Osteogenic stimulation robustly increased OCN level of the ECM, which increase was attenuated by iron, leading to complete inhibition at the concentration of 25 μmol/L or higher (Fig. 3C). Next, we have checked whether the anti-osteogenic effect of iron is selective for Ca and Pi-induced osteogenic differentiation of BMSCs or it is a more general inhibitor of osteogenesis. We triggered osteogenic differentiation with a mixture of dexamethasone, ascorbic acid and β-glycerolphosphate in the presence or absence of iron (50 μmol/L). Osteogenic mixture induced a 3.4 ± 0.86-fold, and a 5.75 ± 1.27-fold increase in Runx2 mRNA level on day7 and day14 respectively (Fig. 3D). In contrast, when osteogenic mixture was applied in the presence of iron, mRNA level of Runx2 stayed on the level of unstimulated cells (Fig. 3D). Additionally, we evaluated whether iron inhibits osteogenic mixture-induced

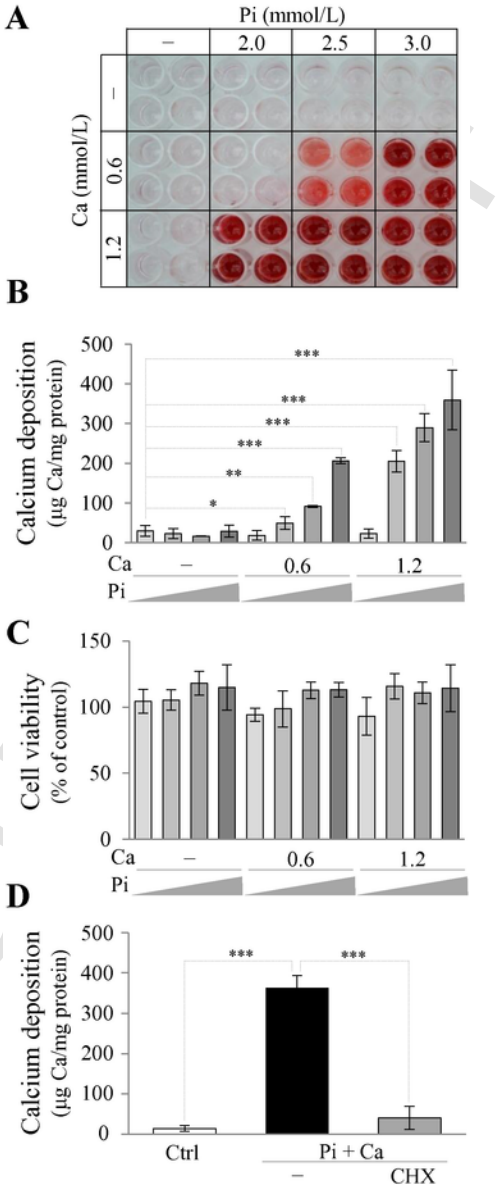

Fig. 1. Pi and Ca induce mineralization of BMSCs in a dose-dependent manner. Confluent BMSCs (passage 5–6) grown in 96-well plates were cultured in growth medium supplemented with Pi (0–3 mmol/L) and Ca (0–1.2 mmol/L) as indicated for 5 days. (A) Ca deposition as a readout of ECM mineralization was visualized by alizarin red staining. Representative image of stained plates from three independent experiments is shown. (B) Ca content of HCl-solubilized ECM is shown. Data are expressed as mean ± S.D. of three independent experiments performed in quadruplicates.*$p < 0.05$, **$p < 0.01$, ***$p < 0.005$. (C) Cell viability was determined by MTT assay after 5 days of osteogenic treatment. Data represent mean ± S.D. of three independent experiments performed in quadruplicates. (D) Confluent BMSCs were cultured under control (Ctrl) or osteogenic conditions (3 mmol/L Pi, and 1.2 mmol/L Ca) in the absence or presence of cycloheximide (CHX, 10 μg/mL) for 5 days. Ca content of HCl-solubilized ECM is shown. Results are expressed as mean ± S.D. of three independent experiments performed in triplicates. ***$p < 0.005$.

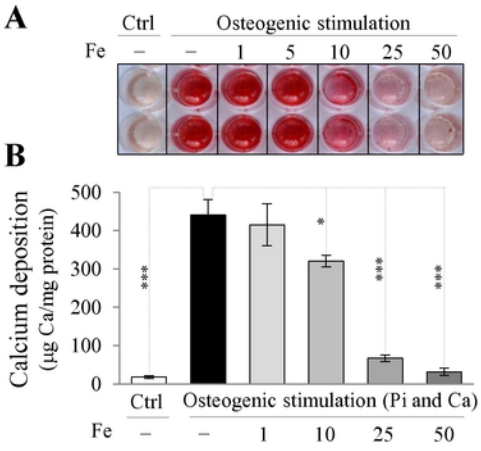

Fig. 2. Iron inhibits Pi and Ca-induced mineralization of BMSCs in a dose-dependent manner. (A–B) Confluent BMSCs (passage 4–6) were cultured under control (Ctrl) or osteogenic conditions (3 mmol/L Pi, and 1.2 mmol/L Ca) in the absence or presence of iron (0–50 μmol/L) for 5 days. (A) Ca deposition as a readout of ECM mineralization was visualized by alizarin red staining. Representative image of stained plates from three independent experiments is shown. (B) Ca content of HCl-solubilized ECM is shown. Results are expressed as mean ± S.D. from three independent experiments performed in triplicates.*$p < 0.05$, ***$p < 0.005$.

increase of ALP activity. Osteogenic mixture consisted of dexamethasone, ascorbic acid and β-glycerolphosphate induced a marked elevation of ALP activity (4.76 ± 0.36 vs. 16.59 ± 1.69 unit/mg protein) in BMSCs. Increase of ALP activity triggered by osteogenic mixture was reduced by about 40% in the presence of iron (Fig. 3E).

3.4. Ferritin mimics the effect of iron in inhibiting ECM mineralization of BMSCs

Previously we found that iron inhibits VSMC osteogenic trans-differentiation and osteoblast activity, via the induction of ferritin [26,31]. Our next question was whether the induction of ferritin is responsible for the anti-osteogenic effect of iron in BMSCs. As expected we found that iron induce a dose-dependent increase in both subunits of ferritin, FtH and FtL (Fig. 4A). Then we challenged BMSCs with osteogenic stimulation in the presence of ferritin at the concentrations of 1 and 2 mg/mL. Alizarin red staining revealed that ferritin strongly inhibited ECM mineralization of BMSCs (Fig. 4B). This result was confirmed by measuring Ca content of the ECM (Fig. 4C).

3.5. Ferritin mimics the effect of iron in down-regulating Runx2, OCN and ALP

To examine whether inhibition of ECM mineralization by ferritin is associated with failed increase in the expression of Runx2 upon osteogenic stimuli, we measured Runx2 mRNA and protein expressions in BMSCs challenged with osteogenic medium in the presence or absence of ferritin. Osteogenic stimuli induced an about 2-fold increase in Runx2 mRNA levels when compared to control cells (Fig. 5A).This response was completely abrogated in the presence of ferritin. Western blot analysis revealed that ferritin dose-dependently decreased the expression of Runx2 when compared to stimulated cells (Fig. 5B). Expressions of osteoblast-specific proteins, OCN and ALP are under the control of Runx2, therefore next we examined whether down-regulation of Runx2 is associated with decreased protein levels of these target genes in BMSCs under osteogenic stimulation. We determined OCN levels in the solubilized ECM of BMSCs, and found that OCN levels were very low in ferritin-treated samples (Fig. 5C). Comparison of ALP expressions in BMSCs under osteogenic conditions in the presence or absence of ferritin revealed that ALP expression of ferritin-treated cells was about ten times lower than in the absence of ferritin (Fig. 5D).

3.6. Anti-osteogenic effect of iron and ferritin is independent of phosphate uptake

Phosphate uptake is critical in initiating Pi-mediated osteogenic trans-differentiation of VSMC. To examine whether iron or ferritin influence BMSC phosphate uptake, we assessed intracellular phosphate levels in unstimulated and stimulated cells, in the presence or absence of iron and ferritin. Osteogenic stimuli increased intracellular Pi levels of BMSCs about 1.5-fold over unstimulated cells (Fig. 6A). Importantly neither iron nor ferritin treatment influenced phosphate uptake of BMSCs, suggesting that other mechanism(s) are behind the anti-osteogenic effect of both iron and ferritin (Fig. 6A).

3.7. Iron overload increase ROS production in BMSCs, but increased ROS production is not responsible for impaired osteogenesis

Considering that iron is involved in ROS generation, and that ROS are recognized as critical factor in osteogenic differentiation of BMSCs, next we examined the effect of osteogenic stimuli on ROS levels in the presence or absence of iron and ferritin. We followed ROS generation for 3 h in BMSCs after a 24-hour osteogenic stimulation. Osteogenic stimulation decreased ROS generation when compared to non-stimulated cells (Fig. 6B). Interestingly, both iron and ferritin inhibited osteogenic stimuli-induced decrease in ROS generation in BMSCs, which resulted that ROS productions in iron or ferritin-treated stimulated cells were similar to that of non-calcifying control cells (Fig. 6B). Then we applied the ROS scavenger NAC and looked at whether osteogenic potential of iron-treated cells can be restored by scavenging excess ROS. NAC at the dose of 0.5 mmol/L was able to completely scavenge iron-mediated excessive production of ROS (Fig. 6C). To see whether scavenging excess ROS in iron-treated BMSCs could restore osteogenic ability of BMSCs, we cultured cells in osteogenic medium alone or in the presence of Fe (50 μmol/L) and NAC (0.5 mmol/L) for 5 days. Alizarin red staining revealed that mineralization did not occur in the co-presence of Fe and NAC (Fig. 6D). This finding was confirmed by measuring Ca content of the HCl-solubilized ECM (Fig. 6E).

3.8. Iron overload downregulates the expression of Runx2 in OPCs in vivo

To investigate whether excess iron reduce osteogenic potential of OPCs in vivo, we induced iron-overload condition in C57BL/6 mice and measured mRNA level of the key osteogenic transcription factor, Runx2 and the iron storage protein FtH in compact bone-derived OPCs. As we expected iron overload caused a marked increase (4.52 ± 2.07-fold) in FtH mRNA level, which was associated with a 60% decrease in Runx2 mRNA level in OPCs.

3.9. Iron does not influence either chondrogenic or adipogenic differentiation of BMSCs

BMSCs are multipotent cells, with the ability to differentiate into chondrocytes as well. To examine whether iron can influence chondrogenic differentiation, we cultured BMSCs in chondrogenic medium, supplemented with iron for 14 days. As revealed by Alcian

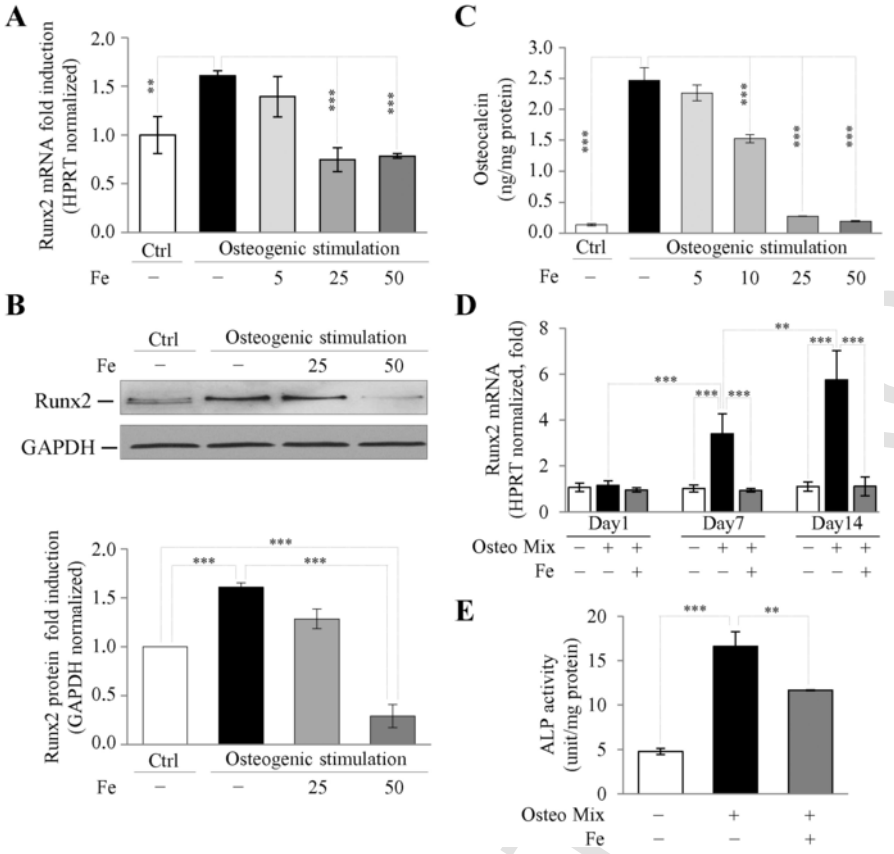

Fig. 3. Iron inhibits osteogenic stimuli-induced upregulation of Runx2 and OCN. (A–C) Confluent BMSCs (passage 6–7) grown in 6-well plates were treated with osteogenic medium supplemented with iron at the indicated concentrations (0–50 μmol/L) for 5 days. (A) Runx2 mRNA levels were determined by real time RT-PCR. Results are presented as mean ± S.D. of three independent experiments performed in triplicates. $^{**}p < 0.01$, $^{***}p < 0.005$. (B) Representative Western blots from three independent experiments are shown. Relative expressions of Runx2 normalized to GAPDH were determined by densitometric analysis. Graph shows mean ± S.D. of three independent experiments. (C) ECM of cells was dissolved in 100 μL of EDTA, and OCN content of the obtained samples was quantified by an ELISA. Results are presented as mean ± S.D. of three independent experiments performed in triplicates. $^{***}p < 0.005$. (D) Confluent BMSCs (passage 7) grown in 6-well plates were treated with osteogenic medium supplemented with dexamethasone (0.1 μmol/L), ascorbic acid (50 μmol/L) and β-glycerol-phosphate (2 mmol/L) in the presence or absence of iron (50 μmol/L) for 1, 7 and 14 days. Runx2 mRNA levels were determined by real time RT-PCR. Results are presented as mean ± S.D. of two independent experiments performed in triplicates. $^{**}p < 0.01$, $^{***}p < 0.005$. (E) Confluent BMSCs (passage 7) grown in 96-well plates were treated with osteogenic medium supplemented with dexamethasone (0.1 μmol/L), ascorbic acid (50 μmol/L) and β-glycerol-phosphate (2 mmol/L) in the presence or absence of iron (50 μmol/L) for 1, 7 days. ALP activity was determined by a colorimetric assay and normalized to protein content. Results are presented as mean ± S.D. of two independent experiments performed in quadruplicates. $^{**}p < 0.01$, $^{***}p < 0.005$.

blue staining, iron did not influence chondrogenic differentiation of BMSCs (Fig. 7A). This was confirmed by the determination of the expression of aggrecan, a major component of ECM of cartilaginous tissues. As shown by Western blot, iron treatment did not influence the expression of aggrecan, suggesting that iron had no effect on chondrogenic lineage commitment of BMSCs (Fig. 7B). Finally, we examined the role of iron in the process of adipogenic differentiation of MSCs. We cultured BMSCs in adipogenic medium, in the absence or presence of iron for 33 days. As revealed by Oil Red O staining, iron did not influence adipogenic potential of BMSCs (Fig. 7C). To further confirm that iron has no effect on adipogenesis, we determined mRNA and protein expressions of Fabp4, the adipocyte-specific protein (Fig. 7D–E). We found no effect of iron on Fabp4 mRNA and protein expressions, suggesting that adipogenic lineage commitment is maintained in the presence of iron.

4. Discussion

In this study we used BMSCs to examine the effect of iron in the processes of osteogenic, chondrogenic and adipogenic differentiation. Osteogenic commitment and differentiation of BMSCs has been studied extensively using various stimulants including bone-morphogenetic proteins, dexamethasone, L-ascorbic acid 2-phosphate, and β-glycerolphosphate; being the last three are the most widely used supplements in osteogenic medium [32]. To induce osteogenic differentiation of BMSCs here we applied Pi and Ca, the well-known and pathophysiologically relevant triggers of osteoblastic trans-differentiation of VSMC [33]. We found that the effects of elevated Pi and Ca are synergistic, and when applied together, they caused a robust ECM mineralization, characterized by increased Ca content, and alizarin red-positivity. Mineralization of ECM is much faster in response to Ca and Pi when compared to previously described inducers (5 days vs. 8–14 days), that could be a great advantage in bone tissue-engineering approaches [34].

Many lines of evidence suggested a link between iron overload and decreased bone mass. Excess iron accumulates in the bones of individuals with hemochromatosis [35], and there is a long-known association between hemochromatosis and low bone mineral density [8–11]. In a study of iliac crest biopsies from 21 individuals with severe osteoporosis iron bone concentration was evaluated and a significant increase in iron content in cortical bone was found in osteoporotic patients vs. 12 controls [36]. Recently in a prospective cross-

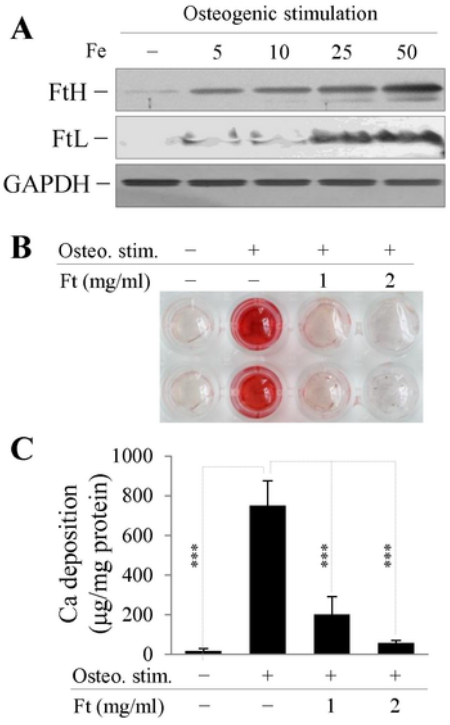

Fig. 4. Ferritin mimics the effect of iron in inhibiting mineralization of BMSCs. (A) Confluent BMSCs (passage 4–5) grown in 6-well plates were treated with osteogenic medium supplemented with iron at the indicated concentrations (0–50 μmol/L) for 5 days. Expressions of ferritin H (FtH) and L (FtL) chains were determined by Western blot. Immunoblots were reprobed with GAPDH and are representative of three independent experiments. (B–C) Confluent BMSCs (passage 4–5) grown in 96-well plates were treated with osteogenic medium in the presence or absence of ferritin (1 and 2 mg/mL) for 5 days. (B) Ca deposition as a readout of ECM mineralization was visualized by alizarin red staining. Representative image of stained plates from three independent experiments is shown. (C) Ca content of HCl-solubilized ECM is shown. Results are expressed as mean ± S.D. from three independent experiments performed in triplicates. ***$p < 0.005$.

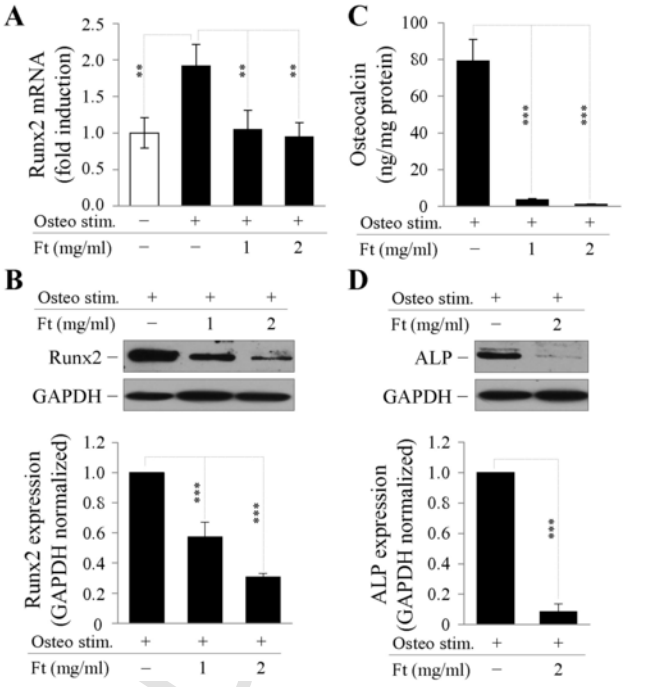

Fig. 5. Ferritin abrogates osteogenic stimuli-mediated up-regulation of Runx2, OCN and ALP in BMSCs. Confluent BMSCs (passage 6–7) grown in 6-well plates were treated with osteogenic medium in the presence or absence of ferritin as indicated for 5 days. (A) Relative Runx2 level normalized to HPRT was determined by quantitative RT-PCR. Results are expressed as mean ± S.D. from three independent experiments performed in triplicates. **$p < 0.01$. (B) Representative Western blots from three independent experiments are shown. Relative expressions of Runx2 normalized to GAPDH were determined by densitometric analysis. Graph shows mean ± S.D. of three independent experiments. (C) ECM of cells was dissolved in 100 μL of EDTA, and OCN was quantified by ELISA. Results are expressed as mean ± S.D. of three independent experiments. ***$p < 0.005$. (D) Expression of ALP was determined by Western blot from whole cell lysate. Representative Western blots from three independent experiments are shown. Relative expressions of ALP normalized to GAPDH were determined by densitometric analysis. Graph shows mean ± S.D. of three independent experiments.

sectional study on 80 patients with beta thalassemia major and intermedia, the authors found that both serum ferritin and heart iron load were negatively correlated with bone mineral density [37]. Animal models of iron overload also supported the deleterious effect of excess iron on bone mineral density [12–14,16,38,39].

Bone is a dynamic, highly vascularized tissue with a unique repair capacity to heal and remodel without scarring. The remodeling process is orchestrated mainly by osteoclasts, responsible for bone resorption, and osteoblasts that build up the new bone tissue [40]. Osteoclasts differentiate from mononuclear precursors [41], whereas osteoblasts derive from mesenchymal progenitor cells, which migrate to the site of injury, proliferate and differentiate [27]. Considering the complexity of bone remodeling, the deleterious effect of iron on bone physiology can be multifactorial.

The receptor activator of nuclear factor-kappa B ligand (RANKL)/osteoprotegerin (OPG) pathway is the dominant regulator of osteoclast proliferation and activation [42]. Iron has been shown to facilitate RANKL-induced osteoclast formation in both RAW264.7 cells and bone marrow-derived macrophages in an oxidative stress-mediated way [24]. Iron overload conditions are associated with elevated RANKL/OPG [43], whereas the iron-chelating lactoferrin has been shown to improve bone density via decreasing RANKL/OPG ratio [44]. Besides its effect on osteoclast differentiation, iron dramatically influences osteoblast metabolism. Ferric iron has been shown to decrease proliferation and mineralization of MC3T3-E1 osteoblastic cells [45]. Moreover, Zarjou et al. showed that iron down-regulates the expression of osteoblast-specific proteins, such as OCN and ALP, as well as the expression of Runx2, the osteoblast-specific transcription factor in human osteoblasts [26]. The same study highlighted the crucial importance of ferritin in iron-mediated inhibition of osteoblast function [26].

Osteoblasts originate from BMSCs, therefore BMSCs play a pivotal role in bone homeostasis. Recently it has been shown that the number of circulating BMSCs was increased in osteoporotic patients compared to controls, but the cells derived from osteoporotic patients showed decreased osteogenic commitment and differentiation potential [28]. Here we demonstrated that iron is a potent inhibitor of osteogenic differentiation of BMSCs. Iron decreased osteogenic stimuli-triggered ECM mineralization of BMSCs (Fig. 2). In response to osteogenic stimuli, BMSCs increase the expression of Runx2, the key transcription factor involved in osteogenic differentiation. In the presence of iron this response was completely abrogated. Parallel with Runx2, OCN expression and ALP activity were increased in mineralizing ECM, but osteogenic stimuli-triggered elevation of OCN expression and ALP activity were attenuated in the presence of iron (Fig. 3). We also showed that ferritin mimicked the inhibitory effect of iron in BMSC differentiation and mineralization (Figs. 4–5) similarly to that was found in osteoblasts [26]. Additionally, in this work we investigated the in vivo effect of iron on osteogenic potential of

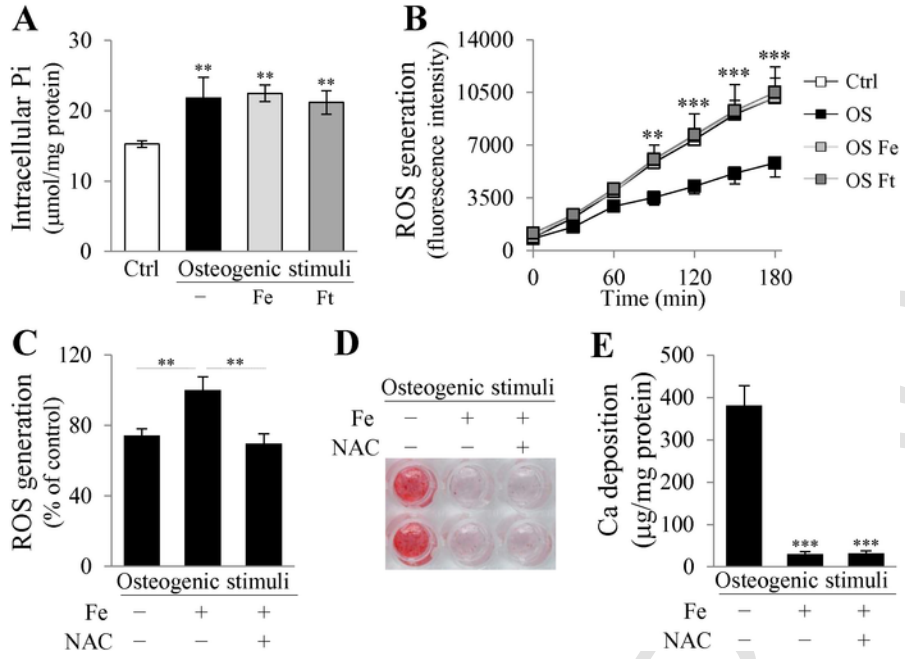

Fig. 6. Iron and ferritin have no effect on phosphate uptake but increase ROS production in BMSCs. (A–B) Confluent BMSCs (passage 6–7) grown in 96-well plates were treated with growth medium or osteogenic medium in the presence or absence of iron (50 μmol/L) or ferritin (2 mg/mL) as indicated, for 24 h. (A) Intracellular phosphate content of cell lysates was determined with phosphate assay kit, in triplicates. Results are shown as mean ± S.D. from one representative experiment of three. $^{**}p < 0.01$. (B) ROS levels were detected for 3 h in every 30 min in triplicates. Results are expressed as mean ± S.D. of three independent experiments. $^{**}p < 0.01$, $^{***}p < 0.005$. (C–D) Confluent BMSCs (passage 7) grown in 96-well plates were treated with osteogenic medium in the presence of iron (50 μmol/L) and NAC (0.5 mmol/L) when labeled. (C) ROS generation was measured 90 min post-stimulation in quadruplicates. Results are shown as mean ± S.D. from one representative experiment of two. $^{**}p < 0.01$. (D) Ca deposition as a readout of ECM mineralization was visualized by alizarin red staining on day5. Representative image of stained plates from three independent experiments is shown. (E) Ca content of HCl-solubilized ECM on day5 is shown. Results are expressed as mean ± S.D. from three independent experiments performed in triplicates. $^{***}p < 0.005$.

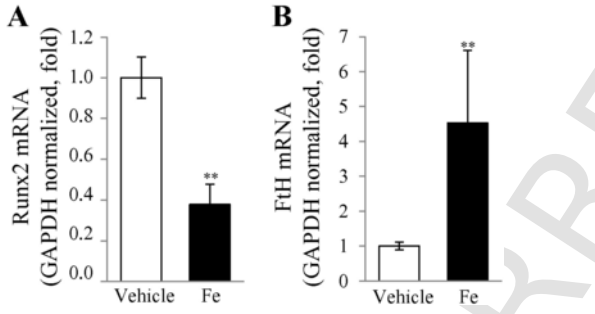

Fig. 7. Iron overload downregulates the expression of Runx2 in compact bone OPCs in vivo. (A–B) C57BL/6 mice were treated with iron-dextran (200 mg/kg, $n = 5$) or vehicle (PBS, $n = 5$) 3 times in every other day. Runx2 and FtH mRNA levels were determined in compact bone-derived OPCs by real time RT-PCR using GAPDH as internal control. Results are presented as mean ± SEM. $^{**}p < 0.01$.

OPCs. We found that Runx2, the key osteogenic transcription factor is markedly downregulated in compact bone OPCs in mice with systemic iron overload (Fig. 7). Our results provide a novel mechanism via which excess iron/ferritin could contribute to osteoporosis by impairing osteogenic differentiation of BMSCs and OPCs.

Several lines of evidence suggested an inverse relationship between osteogenic and adipogenic differentiation of MSCs such that signaling pathways that induce osteogenesis do so at the expense of adipogenesis and the other way around [46]. Therefore we examined the role of iron in adipogenic differentiation of BMSCs expecting that iron may increase adipogenic potential of BMSCs. Interestingly, we found that iron does not influence adipogenesis (Fig. 8), suggesting that the iron/ferritin system is an exception to this rule. Additionally, we described here that iron does not impair chondrogenic differentiation of BMSCs (Fig. 8).

It is currently believed that tightly regulated levels of ROS are crucial in promoting diverse signaling pathways, involved in a wide variety of cellular functions, including differentiation process [7]. For example, excess ROS production has found to be associated with decreased bone formation via the inhibition of diverse signaling pathways, including Wnt, FOXO and Hedgehog signaling in MSCs [7]. Moreover, resveratrol, a natural polyphenol antioxidant was shown to promote osteogenic differentiation of murine pluripotent stem cells [47]. Considering that excess iron is a well-known trigger of intracellular ROS formation, we hypothesized that iron inhibits osteogenic differentiation of BMSCs, via facilitating ROS production. We found that osteogenic differentiation of BMSCs is accompanied by decreased generation of ROS. Additionally, our data revealed that anti-osteogenic activity of iron was associated with increased ROS generation (Fig. 6). On the other hand scavenging excess ROS with NAC could not restore osteogenic potential of iron-treated BMSCs, suggesting that the elevated ROS is not the ultimate inhibitor of the osteogenic differentiation process. Recently it has been shown that osteogenic differentiation of MSCs is accompanied by metabolic changes, upregulation of antioxidant enzymes and a dramatic reduction of intracellular ROS formation [48]. Based on these data we cannot exclude that the observed elevation of ROS production in iron-treated BMSCs is a consequence and not the cause of arrested osteogenesis, which remained to be elucidated in further studies.

Interestingly ferritin, the cytosolic iron storage molecule, mimicked the anti-osteogenic effect of iron. Usually ferritin is considered as an anti-oxidant molecule that can store iron in a redox inactive form, and thus prevents the formation of ROS [49]. But under specific circumstances ferritin can behave as a pro-oxidant molecule. For exam-

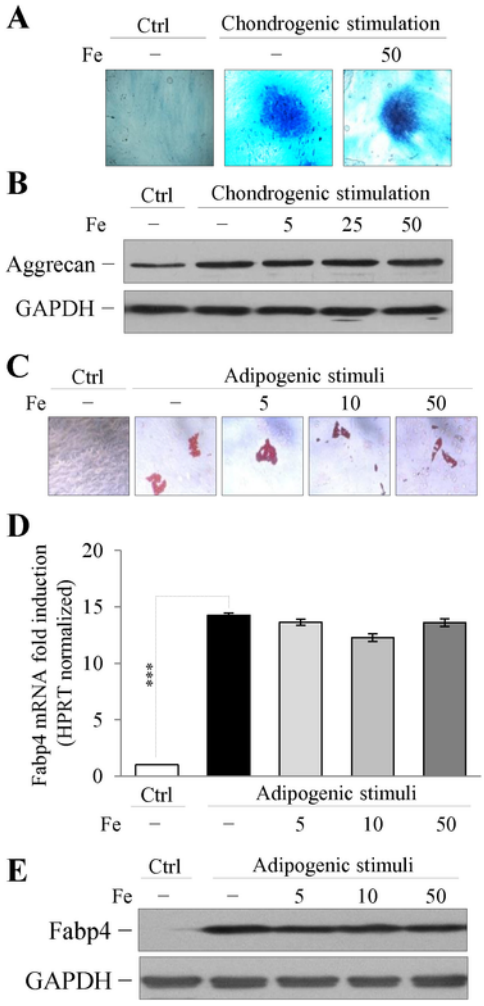

Fig. 8. Chondrogenic and adipogenic differentiation potentials of BMSCs are maintained in the presence of iron. (A–B) Confluent BMSCs (passage 5–6) grown in 6-well plates were cultured in chondrogenic medium supplemented with iron (0–50 μmol/L) for 14 days. (A) Chondrogenic differentiation was visualized by Alcian blue staining. Representative image of stained plates from three independent experiments is shown. (B) Expression of aggrecan was determined by Western blot from whole cell lysate. Immunoblots were reprobed with GAPDH and are representative of three independent experiments. (C–E) Confluent BMSCs (passage 5–6) grown in 6-well plates were cultured in adipogenic medium supplemented with iron (0–50 μmol/L) for 33 days. (C) Adipogenic differentiation was visualized by Oil Red O staining. Representative image of stained plates from three independent experiments is shown. (D) Relative Fabp4 level normalized to HPRT was determined by quantitative RT-PCR. Results are expressed as mean ± S.D. from three independent experiments performed in triplicates. ***$p < 0.005$. (E) Expression of Fabp4 was determined by Western blot from whole cell lysate. Immunoblots were reprobed with GAPDH and are representative of three independent experiments.

ple, artesunate, the anti-malarial drug with anti-tumor activity, was shown to induce cell death via enhancing lysosomal degradation of ferritin [50]. It is becoming accepted that ferritin can behave a pro-oxidant manner when certain trigger molecules can liberate the sequestered iron, or open the gated pores of ferritin [51]. We found elevated ROS production in ferritin-treated BMSCs, suggesting that ferritin behave in a pro-oxidant manner under osteogenic stimulation. Further studies are needed to address whether osteogenic stimulation is a condition in which lysosomal degradation of ferritin occurs.

In conclusion, our findings provide evidence that excess iron specifically inhibits in vitro osteogenic differentiation of BMSCs, via the down-regulation of the key osteogenic transcription factor, Runx2, meanwhile chondrogenic and adipogenic differentiation potentials of BMSCs are maintained. The anti-osteogenic effect of iron is mimicked by exogenously administered ferritin. Importantly, iron overload in mice was associated with increased FtH and decreased Runx2 expressions in compact bone-derived OPCs, suggesting that the described mechanism could have importance in pathological bone loss in iron overload diseases.

Authors contributions

Enikő Balogh: Collection and assembly of data, participation in drafting the manuscript writing, final approval of the submitted manuscript.

Emese Tolnai: Collection and assembly of data, participation in drafting the manuscript writing, final approval of the submitted manuscript.

Béla Nagy Jr.: Acquisition of data, revision and final approval of the manuscript.

Béla Nagy: Conception and design, revision and final approval of the manuscript.

György Balla: Conception and design, revision and final approval of the manuscript.

József Balla: Conception and design, revision and final approval of the manuscript.

Viktória Jeney: Conception and design, data analysis and interpretation, drafting the manuscript, final approval of the manuscript. She is responsible for the integrity of the data analysis.

All authors agree to be accountable for all aspects of the work in ensuring that questions related to the accuracy or integrity of any part of the work are appropriately investigated and resolved.

Disclosure of potential conflicts of interest

The authors declared that no conflict of interest exists.

Transparency document

The Transparency document associated with this article can be found, in the online version.

Acknowledgements

This work was supported by the Hungarian Government grant OTKA-K116024 and the University of Debrecen Research Grant RH/751-2/2015. The project was co-financed by the European Union and the European Social Fund TÁMOP-4.2.4.A/2-11-1-2012-0001. Béla Nagy Jr. was supported by the Lajos Szodoray Grant by the University of Debrecen.

References

[1] G. Chamberlain, J. Fox, B. Ashton, J. Middleton, Concise review: mesenchymal stem cells: their phenotype, differentiation capacity, immunological features, and potential for homing, Stem Cells 25 (11) (2007) 2739–2749.

[2] A.W. James, Review of signaling pathways governing MSC osteogenic and adipogenic differentiation, Scientifica 2013 (2013) 684736.

[3] R.T. Franceschi, G. Xiao, D. Jiang, R. Gopalakrishnan, S. Yang, E. Reith, Multiple signaling pathways converge on the Cbfa1/Runx2 transcription factor to regulate osteoblast differentiation, Connect. Tissue Res. 44 (Suppl. 1) (2003) 109–116.

[4] F. Otto, A.P. Thornell, T. Crompton, A. Denzel, K.C. Gilmour, I.R. Rosewell, et al., Cbfa1, a candidate gene for cleidocranial dysplasia syndrome, is essential for osteoblast differentiation and bone development, Cell 89 (5) (1997) 765–771.

[5] T. Komori, H. Yagi, S. Nomura, A. Yamaguchi, K. Sasaki, K. Deguchi, et al., Targeted disruption of Cbfa1 results in a complete lack of bone formation owing to maturational arrest of osteoblasts, Cell 89 (5) (1997) 755–764.
[6] P. Ducy, R. Zhang, V. Geoffroy, A.L. Ridall, G. Karsenty, Osf2/Cbfa1: a transcriptional activator of osteoblast differentiation, Cell 89 (5) (1997) 747–754.
[7] F. Atashi, A. Modarressi, M.S. Pepper, The role of reactive oxygen species in mesenchymal stem cell adipogenic and osteogenic differentiation: a review, Stem Cells Dev. 24 (10) (2015) 1150–1163.
[8] N.G. Angelopoulos, A.K. Goula, G. Papanikolaou, G. Tolis, Osteoporosis in HFE2 juvenile hemochromatosis. A case report and review of the literature, Osteoporos. Int. 17 (1) (2006) 150–155.
[9] L. Valenti, M. Varenna, A.L. Fracanzani, V. Rossi, S. Fargion, L. Sinigaglia, Association between iron overload and osteoporosis in patients with hereditary hemochromatosis, Osteoporos. Int. 20 (4) (2009) 549–555.
[10] P. Guggenbuhl, Y. Deugnier, J.F. Boisdet, Y. Rolland, A. Perdriger, Y. Pawlotsky, et al., Bone mineral density in men with genetic hemochromatosis and HFE gene mutation, Osteoporos. Int. 16 (12) (2005) 1809–1814.
[11] L. Sinigaglia, S. Fargion, A.L. Fracanzani, L. Binelli, N. Battafarano, M. Varenna, et al., Bone and joint involvement in genetic hemochromatosis: role of cirrhosis and iron overload, J. Rheumatol. 24 (9) (1997) 1809–1813.
[12] J. Tsay, Z. Yang, F.P. Ross, S. Cunningham-Rundles, H. Lin, R. Coleman, et al., Bone loss caused by iron overload in a murine model: importance of oxidative stress, Blood 116 (14) (2010) 2582–2589.
[13] H. Kudo, S. Suzuki, A. Watanabe, H. Kikuchi, S. Sassa, S. Sakamoto, Effects of colloidal iron overload on renal and hepatic siderosis and the femur in male rats, Toxicology 246 (2–3) (2008) 143–147.
[14] P. Guggenbuhl, P. Fergelot, M. Doyard, H. Libouban, M.P. Roth, Y. Gallois, et al., Bone status in a mouse model of genetic hemochromatosis, Osteoporos. Int. 22 (8) (2011) 2313–2319.
[15] T. Ganz, Systemic iron homeostasis, Physiol. Rev. 93 (4) (2013) 1721–1741.
[16] L. Sun, W. Guo, C. Yin, S. Zhang, G. Qu, Y. Hou, et al., Hepcidin deficiency undermines bone load-bearing capacity through inducing iron overload, Gene 543 (1) (2014) 161–165.
[17] S. Puntarulo, Iron, oxidative stress and human health, Mol. Asp. Med. 26 (4–5) (2005) 299–312.
[18] P.M. Harrison, P. Arosio, The ferritins: molecular properties, iron storage function and cellular regulation, Biochim. Biophys. Acta 1275 (3) (1996) 161–203.
[19] E.C. Theil, Ferritin: structure, gene regulation, and cellular function in animals, plants, and microorganisms, Annu. Rev. Biochem. 56 (1987) 289–315.
[20] P. Rucker, F.M. Torti, S.V. Torti, Role of H and L subunits in mouse ferritin, J. Biol. Chem. 271 (52) (1996) 33352–33357.
[21] Y. Yoshino, J. Manis, D. Schachter, Regulation of ferritin synthesis in rat liver, J. Biol. Chem. 243 (11) (1968) 2911–2917.
[22] M.W. Hentze, T.A. Rouault, S.W. Caughman, A. Dancis, J.B. Harford, R.D. Klausner, A cis-acting element is necessary and sufficient for translational regulation of human ferritin expression in response to iron, Proc. Natl. Acad. Sci. U. S. A. 84 (19) (1987) 6730–6734.
[23] J.L. Casey, M.W. Hentze, D.M. Koeller, S.W. Caughman, T.A. Rouault, R.D. Klausner, et al., Iron-responsive elements: regulatory RNA sequences that control mRNA levels and translation, Science 240 (4854) (1988) 924–928.
[24] P. Jia, Y.J. Xu, Z.L. Zhang, K. Li, B. Li, W. Zhang, et al., Ferric ion could facilitate osteoclast differentiation and bone resorption through the production of reactive oxygen species, J. Orthop. Res. 30 (11) (2012) 1843–1852.
[25] M. Nouraie, K. Cheng, X. Niu, E. Moore-King, M.F. Fadojutimi-Akinsi, C.P. Minniti, et al., Predictors of osteoclast activity in patients with sickle cell disease, Haematologica 96 (8) (2011) 1092–1098.
[26] A. Zarjou, V. Jeney, P. Arosio, M. Poli, E. Zavaczki, G. Balla, et al., Ferritin ferroxidase activity: a potent inhibitor of osteogenesis, J. Bone Miner. Res. 25 (1) (2010) 164–172.
[27] C. Maes, T. Kobayashi, M.K. Selig, S. Torrekens, S.I. Roth, S. Mackem, et al., Osteoblast precursors, but not mature osteoblasts, move into developing and fractured bones along with invading blood vessels, Dev. Cell 19 (2) (2010) 329–344.
[28] L. Dalle Carbonare, M.T. Valenti, M. Zanatta, L. Donatelli, C.V. Lo, Circulating mesenchymal stem cells with abnormal osteogenic differentiation in patients with osteoporosis, Arthritis Rheum. 60 (11) (2009) 3356–3365.
[29] H. Zhu, Z.K. Guo, X.X. Jiang, H. Li, X.Y. Wang, H.Y. Yao, et al., A protocol for isolation and culture of mesenchymal stem cells from mouse compact bone, Nat. Protoc. 5 (3) (2010) 550–560.
[30] V. Jeney, J. Balla, A. Yachie, Z. Varga, G.M. Vercellotti, J.W. Eaton, et al., Pro-oxidant and cytotoxic effects of circulating heme, Blood 100 (3) (2002) 879–887.
[31] A. Zarjou, V. Jeney, P. Arosio, M. Poli, P. Antal-Szalmas, A. Agarwal, et al., Ferritin prevents calcification and osteoblastic differentiation of vascular smooth muscle cells, J. Am. Soc. Nephrol. 20 (6) (2009) 1254–1263.
[32] N. Jaiswal, S.E. Haynesworth, A.I. Caplan, S.P. Bruder, Osteogenic differentiation of purified, culture-expanded human mesenchymal stem cells in vitro, J. Cell. Biochem. 64 (2) (1997) 295–312.
[33] C.M. Shanahan, M.H. Crouthamel, A. Kapustin, C.M. Giachelli, Arterial calcification in chronic kidney disease: key roles for calcium and phosphate, Circ. Res. 109 (6) (2011) 697–711.
[34] R. Siddappa, H. Fernandes, J. Liu, C. van Blitterswijk, J. de Boer, The response of human mesenchymal stem cells to osteogenic signals and its impact on bone tissue engineering, Curr. Stem Cell Res. Ther. 2 (3) (2007) 209–220.
[35] H. Laeng, T. Egger, C. Roethlisberger, H. Cottier, Stainable bone iron in undecalcified, plastic-embedded sections. Occurrence in man related to the presence of "free" iron?, Am. J. Pathol. 131 (2) (1988) 344–350.
[36] M.F. Basle, Y. Mauras, M. Audran, P. Clochon, A. Rebel, P. Allain, Concentration of bone elements in osteoporosis, J. Bone Miner. Res. 5 (1) (1990) 41–47.
[37] L. Ebrahimpour, S. Akhlaghpoor, A. Azarkayvan, M. Salehi, A. Morteza, R. Alinaghi, Correlation between bone mineral densitometry and liver/heart iron overload evaluated by quantitative T2* MRI, Hematology 17 (5) (2012) 297–301.
[38] M.C. de Vernejoul, A. Pointillart, C.C. Golenzer, C. Morieux, J. Bielakoff, D. Modrowski, et al., Effects of iron overload on bone remodeling in pigs, Am. J. Pathol. 116 (3) (1984) 377–384.
[39] S. Matsushima, M. Hoshimoto, M. Torii, K. Ozaki, I. Narama, Iron lactate-induced osteopenia in male Sprague–Dawley rats, Toxicol. Pathol. 29 (6) (2001) 623–629.
[40] H.M. Frost, Tetracycline-based histological analysis of bone remodeling, Calcif. Tissue Res. 3 (3) (1969) 211–237.
[41] H.K. Vaananen, T. Laitala-Leinonen, Osteoclast lineage and function, Arch. Biochem. Biophys. 473 (2) (2008) 132–138.
[42] L.C. Hofbauer, C.A. Kuhne, V. Viereck, The OPG/RANKL/RANK system in metabolic bone diseases, J. Musculoskelet. Nueronal Interact. 4 (3) (2004) 268–275.
[43] N. Morabito, A. Gaudio, A. Lasco, M. Atteritano, M.A. Pizzoleo, M. Cincotta, et al., Osteoprotegerin and RANKL in the pathogenesis of thalassemia-induced osteoporosis: new pieces of the puzzle, J. Bone Miner. Res. 19 (5) (2004) 722–727.
[44] J.M. Hou, Y. Xue, Q.M. Lin, Bovine lactoferrin improves bone mass and microstructure in ovariectomized rats via OPG/RANKL/RANK pathway, Acta Pharmacol. Sin. 33 (10) (2012) 1277–1284.
[45] K. Yamasaki, H. Hagiwara, Excess iron inhibits osteoblast metabolism, Toxicol. Lett. 191 (2–3) (2009) 211–215.
[46] J.M. Gimble, M.E. Nuttall, The relationship between adipose tissue and bone metabolism, Clin. Biochem. 45 (12) (2012) 874–879.
[47] C.L. Kao, L.K. Tai, S.H. Chiou, Y.J. Chen, K.H. Lee, S.J. Chou, et al., Resveratrol promotes osteogenic differentiation and protects against dexamethasone damage in murine induced pluripotent stem cells, Stem Cells Dev. 19 (2) (2010) 247–258.
[48] C.T. Chen, Y.R. Shih, T.K. Kuo, O.K. Lee, Y.H. Wei, Coordinated changes of mitochondrial biogenesis and antioxidant enzymes during osteogenic differentiation of human mesenchymal stem cells, Stem Cells 26 (4) (2008) 960–968.
[49] P. Arosio, R. Ingrassia, P. Cavadini, Ferritins: a family of molecules for iron storage, antioxidation and more, Biochim. Biophys. Acta 1790 (7) (2009) 589–599.
[50] N.D. Yang, S.H. Tan, S. Ng, Y. Shi, J. Zhou, K.S. Tan, et al., Artesunate induces cell death in human cancer cells via enhancing lysosomal function and lysosomal degradation of ferritin, J. Biol. Chem. 289 (48) (2014) 33425–33441.
[51] R.K. Watt, The many faces of the octahedral ferritin protein, Biometals 24 (3) (2011) 489–500.